THE JOURNAL OF PHYSICAL CHEMISTRY C
A JOURNAL OF THE AMERICAN CHEMICAL SOCIETY

pubs.acs.org/JPCC

Article

Temperature Dependent Carrier Dynamics in Ga-Alloyed CdSe/ZnS Core−Shell Quantum Dots

Krisztina Sárosi, Christopher Tuinenga, Gergely F. Samu, Károly Mogyorósi, Júlia Dudás, Bálint Tóth, Péter Jójárt, Barnabás Gilicze, Imre Seres, Zsolt Bengery, Csaba Janáky, and Viktor Chikán*

Cite This: J. Phys. Chem. C 2024, 128, 3815−3823

Read Online

ACCESS | Metrics & More | Article Recommendations | Supporting Information

ABSTRACT: In this work, temperature dependent transient absorption spectroscopy measurements are presented on gallium-alloyed CdSe/ZnS core−shell nanoparticles between 30 and 130 °C. To our knowledge, temperature dependent measurements in these systems have been reported only in a few papers, although all processes related to carrier recombination are affected by temperature. For these experiments, gallium-alloyed CdSe/ZnS QD samples were used with nominal doping percentages of 2.5%, 7.5%, 15%. The experimental results show that the transient absorption decay is faster for the pristine CdSe/ZnS samples than in the gallium-alloyed samples at all temperatures. It is assumed that Ga-alloying promotes the formation of trions in the samples by introducing occupied impurity levels within the bandgap of CdSe. The resulting Coulomb blockade will, in turn, prolong the hot-electron relaxation process. By variation of the temperature, the distribution of charge carriers in the different recombination channels can be altered to accelerate recombination in the Ga-alloyed samples at higher temperatures. These measurements demonstrated their usefulness for observing the redistribution of charge carriers among different relaxation pathways.

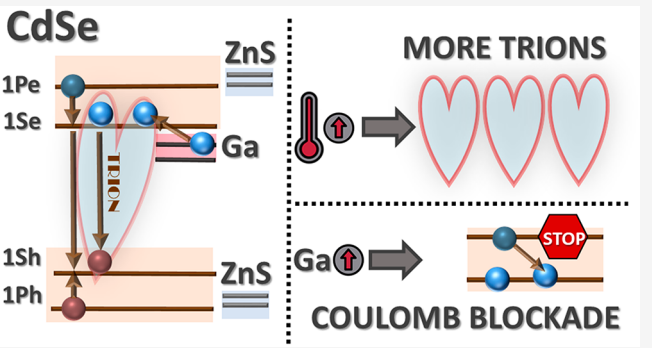

INTRODUCTION

Cadmium chalcogenide nanocrystals and quantum dots (QDs) such as CdS and CdSe have gained significant research interest during the past few decades due to their unique optical, mechanical, magnetic, and catalytic properties.[1−6] These QD systems represent some of the most widely studied and understood QDs in the literature, which is why they are chosen as a host for fundamental doping studies on QDs. The direct measurement of the evolution and decay of the excited states in these systems has helped to better understand the underlying fundamental physical processes of carrier dynamics in semiconductors[7,8] (e.g., different types of recombination and trapping). Introduction of different elements in the lattice of QDs (doping or alloying) results in the modification of the physicochemical properties (e.g., size, energy levels, surface termination of QDs, conductivity, Fermi energy, etc.), which ultimately affects the observed properties of the excited state.[9−12] This modification allows for the fine-tuning of the light emission and absorption properties of the QDs,[13−15] which makes them especially interesting in light harvesting and emission applications.[16,17]

CdSe QDs possess rich excited-state dynamics, with exotic quasi-particles (e.g., dark, bright excitons, trions), where several intertwined processes can occur.[18−22] This is partially caused by the electronic structure of CdSe, where both the conduction and valence bands (CB and VB) are formed from the Cd 5s and Se 4p orbitals.[23] After excitation, the holes have both spin and angular momentum. These properties are also transferred to the formed quasi-particles; thus, optically allowed and forbidden transitions coexist.[19] This already complex picture is further complicated in QD systems, where the large surface-to-volume ratio promotes surface trapping. This trapping process is size dependent and occurs faster in smaller QDs because of the larger charge carrier overlap with the surface.[24] After excitation, the intraband relaxation of holes is coupled to the thermalization of electrons, where the initial hole relaxation occurs in the range of 500 fs−2 ps, depending on QD size but independent of surface properties. Typically hole trapping occurs in the first few picoseconds after excitation and electron trapping in 20−50 ps in CdSe nanocrystals.

Influencing and understanding the dynamics of the short-lived hot carrier population are vital to breaking the efficiency

Received: July 12, 2023
Revised: December 18, 2023
Accepted: December 20, 2023
Published: February 27, 2024

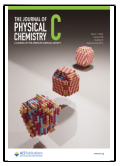

limit of conventional solar cells.[25−28] These hot carriers rapidly relax (subpicoseconds) through various scattering events (carrier−carrier, carrier−phonon, or carrier−impurity), which makes their extraction quite challenging. Prolonging hot carrier lifetime in these materials is either possible through (i) using high excitation densities[29,30] or (ii) utilizing different bottleneck or blockade effects.[20,31] The former strategy (i.e., hot-phonon bottleneck) was recently utilized in lead halide perovskites to achieve longer hot electron lifetimes.[32−36] In the case of Cd chalcogenides, the band structure with the various selection rules allows to prolong carrier lifetimes by forming blockade events (e.g., spin, Coulomb blockade) or by encouraging the formation of exotic quasi-particles (e.g., trions) that have a longer lifetime.[19] These processes require additional electron density in the band structure of the semiconductor, as multiple carriers participate in them. Doping or alloying CdSe QDs with "foreign" (nonnative elements to the host) elements (e.g., Sn, In, Ga, Cu)[7,10,37−40] can introduce filled states within the bandgap of the semiconductor, which in turn can significantly alter the decay of the excited state. Colloidal QDs with n-doped character can be potentially used for harvesting hot electrons.[7] Depending on the foreign element used, markedly different energy levels can be introduced into the semiconductor band structure. In the case of Sn- or In-doped CdSe QDs, the introduced donor electrons are not excited into the CB at room temperature.[7,10,38] In stark contrast with Ga doping, an increased donor electron occupation can be observed even close to room temperature.[41] It has also been demonstrated that Ga-doped CdSe QDs have stronger temperature dependent photoluminescence quenching and a shortened excitonic lifetime due to the increased dopant ionization above room temperature.[10] CdSe QDs with a similar n-type character were also prepared using a photochemical approach in the presence of a hole scavenger under inert atmospheric conditions.[31] Under light doping conditions with above-bandgap excitation, the presence of a Pauli spin blockade prolongs the hot electron lifetime to ∼10 ps. In these cases, an electron already preoccupies the $1S_e$ state in the CB of CdSe. When resonant light excitation is used, the decay of the developing trions can be separated, revealing a characteristic lifetime of ∼460 ps. This lifetime agrees well with that of PL lifetime measurements (in the range of 740 ps).[42] In the case of higher-level doping, the $1S_e$ state is completely filled by two electrons, and the resulting Coulomb blockade further increases the hot-electron lifetime to 300 ps. It is worth noting that not only filled midgap states but also unfilled energy levels can be introduced into the CdSe band structure. By using Cu^+ doping, the hot-electron lifetime is prolonged from ∼0.25 to ∼8.6 ps in doped CdSe QDs.[40] In this case, the introduced impurity level lies closer to the VB of the semiconductor and participated in the hole capture process. In this manner, electrons are efficiently decoupled from the holes, and hot electron relaxation is inhibited.

In this work, we present temperature dependent transient absorption spectroscopy (TAS) measurements on different Ga-alloyed CdSe/ZnS core−shell nanoparticles. In these experiments, we used Ga-alloyed CdSe/ZnS QD samples synthesized in a previous report with nominal doping percentages of 2.5%, 7.5%, and 15%.[9] By altering the Ga content of the sample, we evaluated the effect of dopant density on the mechanism of excited-state decay. The population of the impurity state introduced by gallium can be altered by changing the temperature. In this manner, we also performed temperature dependent TAS measurements in the 30−130 °C range. To the best of our knowledge, temperature dependent measurements in these systems have been reported only in a few papers, although processes related to carrier recombination can all be affected by temperature.[43] Most of these studies focus on the low temperature regime (e.g., −113 to 21 °C).[43] We show how transient absorption spectroscopy performed at higher temperatures can expand our understanding of processes related to the redistribution of carrier populations in doped/alloyed semiconductors.

MATERIALS AND METHODS

Chemicals. The chemicals were used as purchased except for hexadecylamine (HDA), tri-*n*-octylphosphine (TOP), and tri-*n*-octylphosphine oxide (TOPO), which were purified by distillation at 2 Torr. $GaCl_3$, diethylzinc, hexamethyldisilithiane, and tri-*n*-octylphosphine (TOP) were stored in an inert atmosphere glovebox. Toluene (spectrosol grade, Carlo Erba) and xylene (mixture of isomers, Lach-ner) were used for diluting the samples that were frozen in HDA. The $Li_4[Cd_{10}Se_4(SPh)_{16}]$ single source precursor was prepared according to Cumberland's method.[44]

Synthesis of the CdSe Core. Ga-alloyed and pure CdSe core particles were synthesized from the $Li_4[Cd_{10}Se_4(SPh)_{16}]$ single source precursor (SSP) in HDA with $GaCl_3$ as the doping agent.[26] During the process, 50 g of distilled HDA and 0.6 g of the SSP were loaded into a three-neck flask and transferred into a glovebox, where $GaCl_3$ was added. The load percentages of foreign elements (2.5 at. %) are generally based on the total cadmium content of the reaction. In our case, the reaction flask was purged on an Ar gas line for 20 min before gradually being heated to 120 °C with careful attention made to minimize temperature overshoot. The solution was stirred at 120 °C for 18 h while in situ fluorescence spectra were collected.[25] After 12 h, the temperature was increased to 240 °C, and the particles grew to their final size over 3 h.

ZnS Shell Growth. Zn/S stock solution is prepared by mixing 7 mL of diethylzinc with 1 mL of hexamethyldisilithiane and 32 mL of distilled TOPO.[24,25] TOPO and 2-aminopropanol are used without purification. ZnS shell growth is accomplished as follows: a solution of 2 mL of the Zn/S stock solution diluted with 8 mL of TOPO is dispensed using an automated syringe pump over 30 min followed by shell growth for 1 h at 250 °C. After a successive cooling step, another layer of shell material is grown by repeating the dropwise injection at 250 °C. This sequential shell growth is repeated for a total of four injections. The resulting samples are stored at room temperature and diluted in toluene or xylene for the measurements.

EXPERIMENTAL SETUP

The transient absorption/reflection spectroscopy (TAS/TRS) measurements were performed with a dedicated system at ELI ALPS Research Institute.[45] Figure S1 shows the schematic layout of the experimental setup.

The light source was the HR-1 laser,[46] which is a 100 kHz repetition rate, few-optical cycle laser system generating 6−30 fs pulses centered at 1030 nm wavelength and having approximately 1−2 mJ pulse energy. The laser consists of an ytterbium fiber chirped-pulse amplifier front end (250 W) and two postcompression stages, which compress the initial (270

https://doi.org/10.1021/acs.jpcc.3c04689
J. Phys. Chem. C 2024, 128, 3815−3823

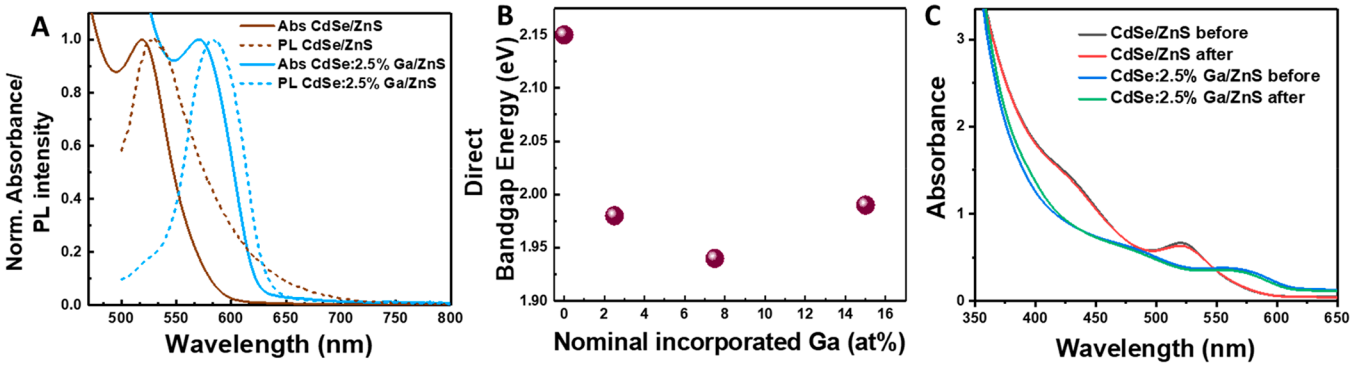

Figure 1. (A) Normalized steady-state UV−vis and PL spectra of CdSe/ZnS and CdSe:2.5%Ga/ZnS QD dispersions. The PL spectra were recorded at a 467 nm excitation wavelength. (B) Determined direct bandgap energies of different Ga-alloyed samples (2.5, 7.5, and 15 at. %). (C) UV−vis absorption spectra of CdSe/ZnS and CdSe:2.5%Ga/ZnS QD dispersion before and after high temperature conditioning (130 °C, t = 1 h).

fs) pulses to 30 fs and finally to 6 fs using the multipass cell technique. With the help of a beam splitter placed after the first postcompression stage, a fraction of the full beam was supplied to the TAS setup. This beam was characterized by 100 μJ pulse energy (10 W average power), 980−1080 nm spectral wavelength, and an approximately transform-limited 30 fs pulse optimized with extra chirp mirrors at the entrance of the experimental setup and measured by a commercial APE PulseCheck autocorrelator. Using a separate power control consisting of a thin-film polarizer and an achromatic half-wave plate, we were able to tune the power between 0 and 10 W in very fine steps, without affecting the spectrum and the pulse duration.

The laser pulse entering the setup was split with a beam splitter (BS) in a ratio of 80/20, where 80% of the beam is used for pump beam generation and the remaining 20% generates the probe beam. The pump beam was frequency-doubled in a Type I BBO crystal (Eksma Optics, 0.2 mm), resulting in a 515 nm center wavelength pulse and compensated for the group-delay-dispersion (GDD) effects of all the transmissive optical elements in the frequency-doubled beam path up to the sample by being reflected 8 times on chirped mirrors (Ultrafast Innovation HD1820). Here the pulse duration was optimized by an autocorrelator (APE PulseCheck-50) with optics for the 400−700 nm wavelength range. Thorlabs' low GDD ultrafast mirrors (UM10-45G) were used to separate the green and infrared beams. The pump beam was focused with an excitation fluence of 0.2 mJ/cm^2 (focal point set to be after the sample), and the probe beam was focused within the cuvette. The white light in the probe path was generated by focusing the beam on a sapphire crystal. On the target, the size of the focused probe beam was 60 × 50 μm^2, and the pump beam was focused behind the sample, ensuring that the focus of the probe beam was smaller than the focus of the pump beam for optimal signal levels and overlap (and that TAS spectra were collected solely in the excited volume of the sample). The pump pulse energy was 1 μJ. The setup contained a high speed (2000 spectra/s) fiber optic Ocean Insight FX spectrometer, which was operated at a 4000 Hz triggering rate and 30 μs integration time. We averaged 2000−5000 spectra with an optical chopper operating at 2000 Hz. The temperature of the samples was controlled with a QPod sample holder. The samples were heated to 130 °C under an argon flow (to avoid any reaction with oxygen at higher temperatures). Before recording the TA spectra, the temperature was allowed to stabilize for at least 5 min while continuous magnetic stirring was used. After the TA spectra were measured, the temperature was decreased to the next value. The maximum usable temperature was dictated by the boiling point of xylene (139.3−144.4 °C). Further attention had to be devoted to keeping the argon flow rate at a sufficiently low level to avoid significant evaporation of the solvent.

During this work, the actual temporal resolution of the instrument at the sample holder, concluded from the TAS measurements, was ∼60 fs, as the transmission optics resulted in a longer pulse duration and slightly worse temporal resolution. The equipment can be quickly switched between the TAS and TRS modes based on the sample or the material to be observed. The main advantage of this setup is the possibility of using different types of sources, which are typically used in pump−probe measurements (1030 nm/515 nm/257 nm−white light/THz).

RESULTS AND DISCUSSION

We prepared CdSe/ZnS core−shell QDs, where the CdSe core was subjected to sequential ZnS shell growth as detailed in our previous study.[9,10] The sequential growth process ensures that the surface traps on CdSe are completely filled and covered with ZnS.[14] The incorporation of the Ga atoms into the CdSe cores takes place prior to the growth of the ZnS shell at a low temperature (120 °C) to minimize self-purification. The introduction of dopant into the synthesis was achieved by the modification of the CdSe synthesis, with addition of the appropriate amount of $GaCl_3$. In this manner, we prepared samples with nominal Ga contents of 2.5, 7.5, and 15.0 at. %. In each case, the role of the ZnS shell was to minimize the contribution of nonradiative recombination to the overall charge carrier dynamics by passivating the surface trap states within these materials.[14] The static UV−vis absorption and PL spectra of the samples were recorded, and the CdSe/ZnS and CdSe:2.5%Ga/ZnS core−shell samples are shown in Figure 1A (other compositions are summarized in Figure S2). From the full-scale UV−vis spectra (Figure S2A), we can observe the features of the ZnS shell on all samples (located around 300 nm). There is a slight blue-shift of this feature with increasing Ga content, which might signal the thinning of the passivating shell with the addition of the Ga into the precursor solution. The static UV−vis absorption spectrum of the CdSe/ZnS sample shows a distinct excitonic peak at 520 nm and a Stokes-shifted emission peak positioned at 530 nm. When 2.5% of Ga was introduced into the CdSe lattice, we observed a significant

https://doi.org/10.1021/acs.jpcc.3c04689
J. Phys. Chem. C 2024, 128, 3815−3823

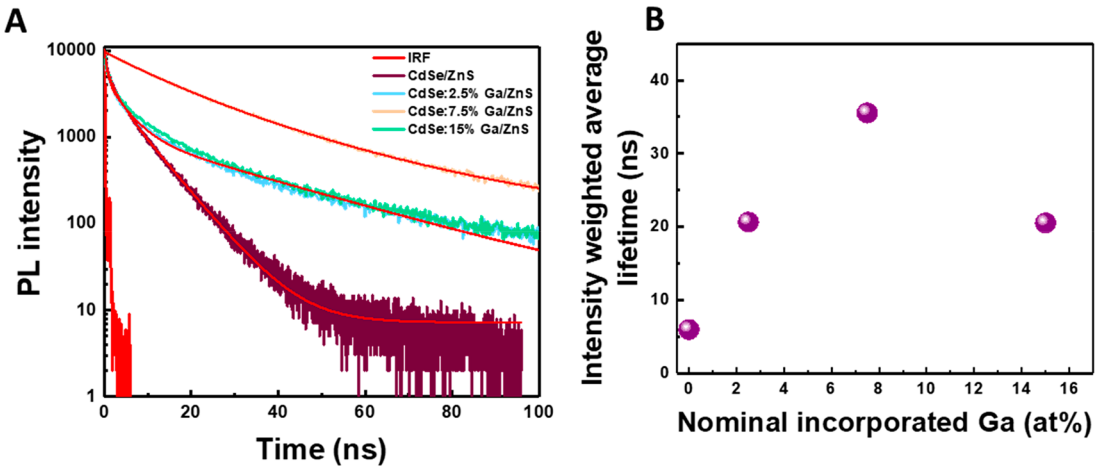

Figure 2. (A) PL decay curves of the CdSe:Ga/ZnS samples. (B) Intensity-weighted average lifetime of the pristine, the CdSe:2.5% Ga/ZnS, the CdSe:7.5% Ga/ZnS, and the CdSe:15% Ga/ZnS samples.

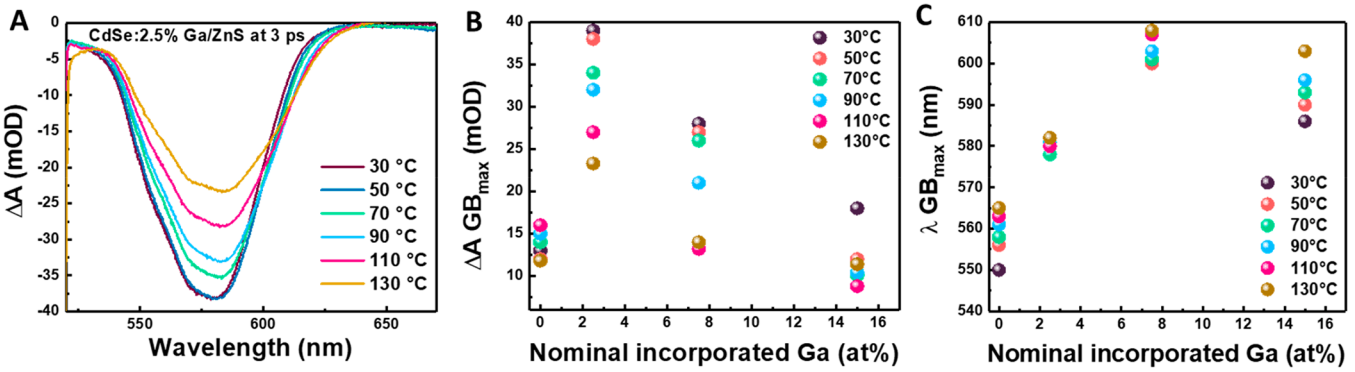

Figure 3. (A) Representative TAS spectra of the CdSe:2.5% Ga/ZnS QDs at different temperatures between 30 and 130 °C at 3 ps, where the maximum GB intensity was observed. (B) Effect of Ga incorporation on the maximum intensity of the bleaching signal for the different samples at different temperatures. (C) Position of the evolved GB peak for the samples at different temperatures.

red-shift of both the absorption and emission features. In the CdSe:2.5% Ga/ZnS sample (Figure S2B,C), the static absorption and the PL peaks were located at 570 and 585 nm, respectively (Figure S2D). This red-shift in the static absorption peak position of the $1S_e-1S_h$ transition was mainly caused by the increasing QD size observed in the HR-TEM images (Figures S3 and S4, Table S1) as shown in Figure S5.[9,10]

The size of the CdSe/ZnS QDs was 3.9 ± 1.6 nm, while the QD diameter of the CdSe:2.5% Ga/ZnS sample was determined to be 4.3 ± 0.9 nm.[9,38] The red-shift appears in the direct bandgap energy of the QD samples (shown in Figure 1B) determined by Tauc analysis.[47,48] This shift seems to saturate above alloying levels of 7.5 at. %. Furthermore, these measurements suggest that the incorporated energy levels related to Ga alloying are occupied, as no additional absorption features are visible on the UV−vis spectra at longer wavelengths (typical of unoccupied midgap states). Interestingly, the 15 at. % Ga-alloyed sample showed an additional peak at lower wavelength values, which is caused by pristine CdSe/ZnS remaining in the dispersion and not by additional transitions (e.g., 1Pe−1Ph transition) promoted by the complete filling of the $1S_e$ energy level.[49] To ensure that the QD samples remain unchanged during the TAS measurements at elevated temperatures, we performed high temperature conditioning (130 °C, t = 1 h) of samples and recorded the UV−vis absorption spectra before and after this step (Figures 1C and S6). It is apparent from these measurements that the optical properties of these samples remained similar, as shown in Figure 1C for the pristine and the CdSe:2.5% Ga/ZnS samples in the temperature range of the TAS measurements presented later.

To gain insights into the effect of Ga-alloying on the PL lifetime of the samples, we performed time-resolved PL measurements that are shown in Figure 2A. We monitored the decay traces at the respective PL peak maxima of the samples. To characterize the average PL lifetime of the samples, the PL decay curves were fitted with a triexponential function. The obtained fitting parameters are summarized in Table S2. The average PL lifetime calculated from these values is shown in Figure 2B. Interestingly, the pristine CdSe/ZnS samples also showed a multiexponential decay, which signals incomplete passivation of the surface trap states in these samples or the contribution of multicarrier processes due to the small size of the QDs. The PL lifetime was significantly shorter in the case of the CdSe/ZnS QDs compared with the measured Ga-containing samples. The longest PL lifetime was observed in the sample containing 7.5 at. % of gallium. Based on the properties of CdSe QDs, this effect can be attributed to the convolution of three separate processes: (i) the addition of the Ga precursor to the synthesis mixture can passivate the surface trap states before the ZnS shell is deposited, (ii) the

https://doi.org/10.1021/acs.jpcc.3c04689
J. Phys. Chem. C 2024, 128, 3815−3823

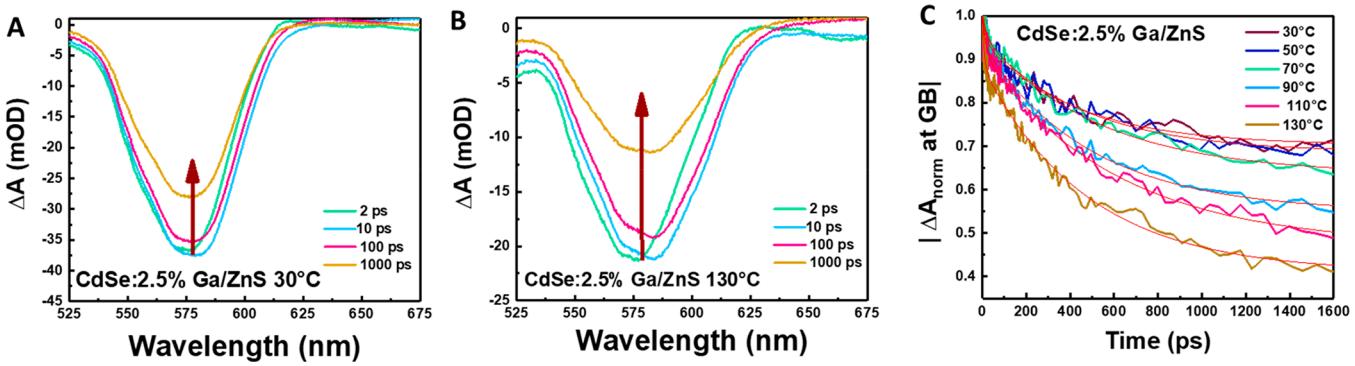

Figure 4. (A) Representative TAS spectra of the CdSe:2.5% Ga/ZnS QDs at 30 °C at different time moments. (B) Representative TAS spectra of the CdSe:2.5% Ga/ZnS QDs at 130 °C at different time moments. (C) Fitted decay trace of the CdSe:2.5% sample at different temperatures.

presence of Ga-related occupied impurity states facilitates the formation of negative trions in these samples, and (iii) size effects related to the increasing CdSe core size with the incorporated Ga. Yet, the length of the PL lifetime is first and foremost determined by increasing QD sizes and the concomitant decrease in trapping depths.[50] Size affects the trion Auger decay in a similar fashion, which explains the longer PL lifetime in Ga-alloyed CdSe QDs.[51]

To observe the effect of Ga incorporation on the processes occurring at short time scales (Figures 3 and S8), we conducted TAS measurements at five different temperatures ranging from 30 to 130 °C in xylene. Prior to the measurements, the absorbance of the samples was adjusted to ∼0.5, and the pump wavelength was set to 515 nm to ensure a similar number of excited carriers in all cases. The representative TAS spectra of the CdSe:2.5% Ga/ZnS QDs at 3 ps (maximum amplitude) at all temperatures can be seen in Figure 3A. We observe little distortion to the shape of the recorded spectra; thus, no additional phases formed during sample heating. However, both Ga alloying and temperature had a pronounced effect on the intensity and position of the ground-state bleach (GB) maximum. Figure 3B shows the extracted maximum intensity of GB of the different samples. As the temperature was increased, the maximum attainable GB intensity dropped in the Ga-alloyed samples. From this we infer that the increase in temperature can promote electrons from the occupied Ga impurity levels to the CB of CdSe QDs. Electrons in the CB can efficiently block the excitation of electrons to the CB edge and thus diminish the bleaching intensity of the samples. An opposite behavior was found for the pristine CdSe samples (Figure 3B) without the Ga impurity levels. In these samples the increasing temperature can promote the $1S_e-1P_e$ excited state transition (0.2 eV).[49] This in turn further increases the population of the excited state, which results in an increase in the magnitude of the GB signal. Note that the change in the absorbance values at the pump wavelength (515 nm) between the 30 and 130 °C spectra was less than 2% for all samples (in the time frame of the TAS measurements), deduced from the steady-state UV−vis spectra (Figure S6). The effect of temperature on the GB intensity in Figure 3B is more significant than the decrease of pump absorption during the measurements. Apart from the maximum GB intensity, the position of the GB was also affected by the incorporation of Ga into the samples (Figure 3C). With increasing Ga content, a similar shift to higher wavelength was observed, as determined from the static UV−vis spectra (Figure 2B). Therefore, we conclude that this can be mainly ascribed to the change in the size of the QDs. Furthermore, at higher temperatures, the GB maximum shifted to higher wavelengths. This shift is in agreement with the temperature dependence of the excitability of semiconductors, where a decrease in the bandgap can be observed with increasing temperature. This in turn will decrease the energy barrier between the Ga-impurity level and the CB edge of CdSe, promoting electron transfer to the CdSe core.

To elucidate how the charge carrier dynamics of the systems is affected by the temperature, we recorded the TAS spectra in the 1−1650 ps time range. The 2D TAS plots for pristine and 2.5% Ga-alloyed CdSe/ZnS samples are shown in Figure S7. These plots suggest that after the evolution of the GB signal no additional features appear in the studied time range. At longer time scales, the steady but incomplete decay of the GB signal is observed. We extracted representative TAS spectra for the CdSe:2.5% Ga/ZnS sample at 30 °C (Figure 4A) and 130 °C (Figure 4B) and also for the pristine sample (shown in Figure S8). These figures clearly indicate that the GB peak decreases more quickly at higher temperatures. Figure 4C shows the decay traces of the CdSe:2.5% Ga/ZnS QDs at different temperatures. As the temperature increases, the GB signal recovers more rapidly. This general tendency was observed for all Ga-alloyed compositions (shown in Figure S9). To elucidate how temperature affects carrier dynamics within these systems, we fitted the curves by a biexponential function (except for the highest Ga content sample). The obtained fitting parameters are summarized in Tables S3−S6. Note that the change in absorbance at the pump wavelength (515 nm) due to temperature is less than 1% throughout the measurements. This continuous decline in absorbance was not considered in the fitting protocol, as sample-to-sample variation has a more pronounced impact on the data.

The decay traces of the CdSe/ZnS QDs showed a multiexponential decay, which is in agreement with the observations from the time-resolved PL measurements. The fast lifetime component (t_1) is attributed to hot-electron relaxation, while the longer lifetime component (t_2) is attributed to the presence of unpassivated trap states within the material. In traditional CdSe QDs the hot-carrier relaxation occurs on the subpicosecond time scales;[49,50] however, in ZnS passivated and/or lightly n-doped CdSe QDs this process can be prolonged to the 10 ps time scales.[31] In the case of n-doped CdSe QDs the electron relaxation process is prolonged by Pauli spin blockade (under lightly doped conditions) and Coulomb blockade (under heavily doped conditions). The presence of additional electrons in Ga-alloyed CdSe QDs

https://doi.org/10.1021/acs.jpcc.3c04689
J. Phys. Chem. C 2024, 128, 3815−3823

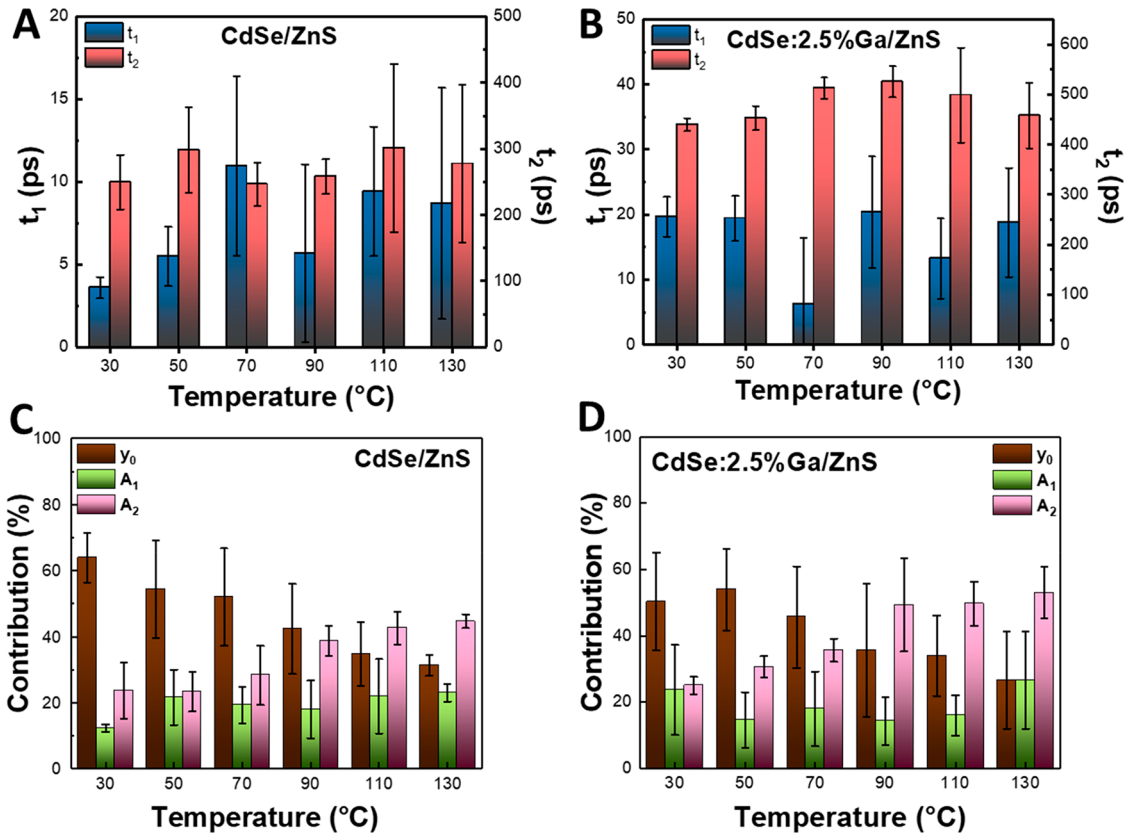

Figure 5. (A) t_1 and t_2 lifetimes of pristine CdSe/ZnS were measured at different temperature levels. (B) t_1 and t_2 lifetimes of CdSe:2.5% Ga/ZnS samples at different temperature levels. (C) Charge carrier contributions of pristine CdSe/ZnS. (D) Charge carrier contributions of CdSe:2.5% Ga/ZnS. The error bars represent measurements on three separate samples.

opens new recombination channels (multicarrier trion decay). This in turn disables the electron-to-hole energy transfer pathway for hot electron relaxation; hence, it can be observed in the decay of the TA signal. It is worth noting that in our measurement window a significant fraction of charge carriers remained separated (y_0), prolonging the recovery of the bleach signal. These charge carriers may participate in radiative recombination channels at longer time scales. The lifetime of the processes seemed to be unaffected by the applied temperature, as shown in Figure 5A. The typical lifetimes were $t_1 \sim 5$ ps and $t_2 \sim 250$ ps in the case of CdSe/ZnS samples at all studied temperatures. Thus, the acceleration of bleach recovery as a result of increasing the temperature was reflected in the contribution of these individual components (A_1, A_2, and y_0) to the overall dynamics (Figure 5C). In these samples, the fraction of charge carriers undergoing trapping increases, diminishing the fraction of carriers available for radiative recombination processes, which is in agreement with the effect of temperature on the PLQY of CdSe QD samples.[52] Significant differences can be observed in the dynamics of Ga-alloyed samples compared to their unalloyed counterpart (Figures 5B and S10). The hot-electron lifetime grew to ~15 ps, while the longer lifetime component also increased to ~500 ps in the CdSe:2.5% Ga/ZnS samples. Interestingly, this longer lifetime component now falls in the lifetime range of trion decay, which is consistent with the incorporation of occupied energy levels of the band structure. A further increase in the individual lifetimes was observed for the CdSe:7.5% Ga/ZnS samples (Figure S10A), where the highly alloyed sample exhibited a monoexponential decay compared to the other samples (Figure S10D,E). This is caused by the short time scale of the TAS measurements, as the longer lifetime component (t_2) now falls outside of the range where it could not be accurately determined by our setup. The proposed mechanism is shown in Scheme 1. A similar temperature

Scheme 1. Schematic Structure of Gallium-Doped CdSe/ZnS Core−Shell Nanoparticles Before and After Heating the Sample

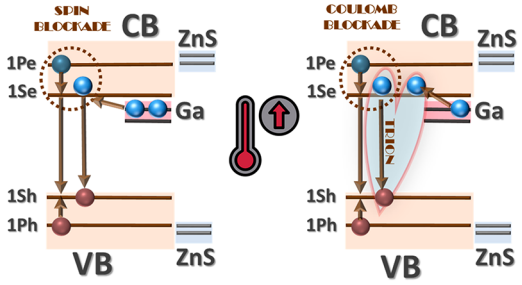

invariance was observed for the lifetimes of these processes (Figure 5B). The acceleration of the decay was also related to the alteration of the population of carriers participating in the individual recovery channels (Figure 5D). A slightly earlier start of the population redistribution can also be observed with Ga-alloying (Figures 5D and S10B,C). To further justify that the temperature increase does not introduce further trap states in the QD samples, we measured the decay traces before and after performing temperature control (Figure S10F). We found that the system showed good reversibility, and the recovery of

https://doi.org/10.1021/acs.jpcc.3c04689
J. Phys. Chem. C 2024, 128, 3815−3823

the excited state was achieved; thus, the observed effects are not related to the temperature instability.

CONCLUSIONS

In summary, we prepared CdSe/ZnS and Ga-alloyed core−shell QDs through the incorporation of different amounts of Ga and characterized their optoelectronic properties with steady-state UV−vis and PL spectroscopy methods. Time-resolved fluorescence measurements showed faster emission decay in unalloyed QDs than in the gallium-alloyed samples. To explore the effect of temperature and Ga incorporation on carrier dynamics in CdSe QDs, we performed temperature dependent TAS measurements. We observed that the recovery of the excited state was faster for the CdSe/ZnS samples compared to that for the gallium-containing samples. Based on our experimental results, we assume that Ga-alloying promotes the formation of trions in the samples, which prolongs the hot-electron lifetime. The temperature had a negligible effect on the determined time constants of the samples; however, it significantly affected the fractions of charge carriers in the different recombination channels. The presented results indicate that temperature dependent TAS measurements are a powerful tool to observe carrier redistribution processes from a variety of relaxation pathways. As an outlook, it is imperative to mitigate the noise during TAS measurements performed at elevated temperatures (e.g., thermal lensing), which is not severe in low temperature scenarios. One potential experimental solution is to consider flow through designs that could potentially alleviate the arising noise.

ASSOCIATED CONTENT

Supporting Information

The Supporting Information is available free of charge at https://pubs.acs.org/doi/10.1021/acs.jpcc.3c04689.

Full-scale static absorption spectra, normalized static absorbance spectra, transmission electron microscopy (TEM) images, size distributions of individual QDs, a table of the determined sizes and their standard deviation, wavelengths of the excitonic feature in respect of the determined QD size, steady-state UV−vis spectra of the QD samples before and after 130 °C heating for 1 h, 2D TAS plots of bleach signals, ground-state bleach spectra of all samples at all temperatures and decay traces of the samples; parameters of the fitted functions: lifetimes and contributions of different processes to the overall decay trace (PDF)

AUTHOR INFORMATION

Corresponding Author

Viktor Chikán − *ELI ALPS, ELI-HU Non-Profit Ltd., H-6728 Szeged, Hungary; Department of Chemistry, Kansas State University, Manhattan, Kansas 66506-0401, United States; ASML, San Diego, California 92127, United States;* orcid.org/0000-0002-4157-3556; Email: vchikan@ksu.edu

Authors

Krisztina Sárosi − *ELI ALPS, ELI-HU Non-Profit Ltd., H-6728 Szeged, Hungary; Department of Optics and Quantum Electronics, University of Szeged, H-6720 Szeged, Hungary*

Christopher Tuinenga − *Department of Chemistry, Kansas State University, Manhattan, Kansas 66506-0401, United States*

Gergely F. Samu − *ELI ALPS, ELI-HU Non-Profit Ltd., H-6728 Szeged, Hungary; Department of Physical Chemistry and Materials Science, Interdisciplinary Excellence Centre, University of Szeged, Szeged H-6720, Hungary;* orcid.org/0000-0002-3239-9154

Károly Mogyorósi − *ELI ALPS, ELI-HU Non-Profit Ltd., H-6728 Szeged, Hungary*

Júlia Dudás − *ELI ALPS, ELI-HU Non-Profit Ltd., H-6728 Szeged, Hungary*

Bálint Tóth − *ELI ALPS, ELI-HU Non-Profit Ltd., H-6728 Szeged, Hungary*

Péter Jójárt − *ELI ALPS, ELI-HU Non-Profit Ltd., H-6728 Szeged, Hungary*

Barnabás Gilicze − *ELI ALPS, ELI-HU Non-Profit Ltd., H-6728 Szeged, Hungary*

Imre Seres − *ELI ALPS, ELI-HU Non-Profit Ltd., H-6728 Szeged, Hungary*

Zsolt Bengery − *ELI ALPS, ELI-HU Non-Profit Ltd., H-6728 Szeged, Hungary*

Csaba Janáky − *ELI ALPS, ELI-HU Non-Profit Ltd., H-6728 Szeged, Hungary; Department of Physical Chemistry and Materials Science, Interdisciplinary Excellence Centre, University of Szeged, Szeged H-6720, Hungary;* orcid.org/0000-0001-5965-5173

Complete contact information is available at: https://pubs.acs.org/10.1021/acs.jpcc.3c04689

Notes

The authors declare no competing financial interest.

ACKNOWLEDGMENTS

The ELI ALPS project (GINOP-2.3.6-15-2015-00001) is supported by the European Union and cofinanced by the European Regional Development Fund. We express our sincere gratitude to Cintia Hajdu (University of Szeged, Hungary) for her support for providing the transmission electron microscopy (TEM) images, to Dr. Veronika Hanyecz (ELI ALPS) for contribution in the UV−vis spectra measurements, and to Rita Emília Szabó (ELI ALPS) and Réka Molnár (ELI ALPS) for their help in the sample preparation. The authors are thankful to Judit Zelena (ELI ALPS) for her language support during the manuscript preparation.

REFERENCES

(1) Hegazy, M. A.; Abd El-Hameed, A. M. Characterization of CdSe-Nanocrystals Used in Semiconductors for Aerospace Applications: Production and Optical Properties. *NRIAG Journal of Astronomy and Geophysics* **2014**, *3* (1), 82−87.

(2) Martinet, Q.; Baronnier, J.; Girard, A.; Albaret, T.; Saviot, L.; Mermet, A.; Abecassis, B.; Margueritat, J.; Mahler, B. Ligand-Dependent Nano-Mechanical Properties of CdSe Nanoplatelets: Calibrating Nanobalances for Ligand Affinity Monitoring. *Nanoscale* **2021**, *13* (18), 8639−8647.

(3) Das, S.; Banerjee, S.; Bandyopadhyay, S.; Sinha, T. P. Magnetic and Dielectric Study of Fe-Doped CdSe Nanoparticles. *Electronic Materials Letters* **2018**, *14* (1), 52−58.

(4) Asere, T. G.; Laing, G. du. Zn-Doped CdSe Nanoparticles: Impact of Synthesis Conditions on Photocatalytic Activity. *Environ. Technol. Innov* **2020**, *20*, No. 101126.

(5) Xiao, J.; Liu, Y.; Steinmetz, V.; Çağlar, M.; Mc Hugh, J.; Baikie, T.; Gauriot, N.; Nguyen, M.; Ruggeri, E.; Andaji-Garmaroudi, Z.;

et al. Optical and Electronic Properties of Colloidal CdSe Quantum Rings. *ACS Nano* **2020**, *14* (11), 14740−14760.
(6) Klimov, V. I.; Ivanov, S. A.; Nanda, J.; Achermann, M.; Bezel, I.; McGuire, J. A.; Piryatinski, A. Single-Exciton Optical Gain in Semiconductor Nanocrystals. *Nature* **2007**, *447* (7143), 441−446.
(7) Roy, S.; Tuinenga, C.; Fungura, F.; Dagtepe, P.; Chikan, V.; Jasinski, J. Progress toward Producing N-Type CdSe Quantum Dots: Tin and Indium Doped CdSe Quantum Dots. *J. Phys. Chem. C* **2009**, *113* (30), 13008−13015.
(8) Hinterding, S. O. M.; Salzmann, B. B. V.; Vonk, S. J. W.; Vanmaekelbergh, D.; Weckhuysen, B. M.; Hutter, E. M.; Rabouw, F. T. Single Trap States in Single CdSe Nanoplatelets. *ACS Nano* **2021**, *15* (4), 7216−7225.
(9) Tuinenga, C. J. *Indium, Tin, And Gallium Doped Cdse Quantum Dots*, 2004.
(10) Luo, H.; Tuinenga, C.; Guidez, E. B.; Lewis, C.; Shipman, J.; Roy, S.; Aikens, C. M.; Chikan, V. Synthesis and Characterization of Gallium-Doped CdSe Quantum Dots. *J. Phys. Chem. C* **2015**, *119* (19), 10749−10757.
(11) Lenngren, N.; Abdellah, M. A.; Zheng, K.; Al-Marri, M. J.; Zigmantas, D.; Žídek, K.; Pullerits, T. Hot Electron and Hole Dynamics in Thiol-Capped CdSe Quantum Dots Revealed by 2D Electronic Spectroscopy. *Phys. Chem. Chem. Phys.* **2016**, *18* (37), 26199−26204.
(12) Honarfar, A.; Mourad, H.; Lin, W.; Polukeev, A.; Rahaman, A.; Abdellah, M.; Chábera, P.; Pankratova, G.; Gorton, L.; Zheng, K.; et al. Photoexcitation Dynamics in Electrochemically Charged CdSe Quantum Dots: From Hot Carrier Cooling to Auger Recombination of Negative Trions. *ACS Appl. Energy Mater.* **2020**, *3* (12), 12525−12531.
(13) Guo, J.; Chen, H.; Zhang, F.; Chen, K.; Wageh, S.; Al-Ghamdi, A. A.; Zhan, H.; He, W.; Wei, S.; Huang, W. Ultrafast Carrier Dynamics in CdS@CdSe Core-Shell Quantum Dot Heterostructure. *Opt Mater. (Amst)* **2022**, *128*, 112367.
(14) Hines, M. A.; Guyot-Sionnest, P. *Synthesis and Characterization of Strongly Luminescing ZnS-Capped CdSe Nanocrystals*, 1996.
(15) Owen, J.; Brus, L. Chemical Synthesis and Luminescence Applications of Colloidal Semiconductor Quantum Dots. *J. Am. Chem. Soc.* **2017**, *139*, 10939−10943.
(16) Barak, Y.; Meir, I.; Shapiro, A.; Jang, Y.; Lifshitz, E. Fundamental Properties in Colloidal Quantum Dots. *Adv. Mater.* **2018**, 1801442.
(17) Pandey, A.; Guyot-Sionnest, P. Slow Electron Cooling in Colloidal Quantum Dots. *Science (1979)* **2008**, *322* (5903), 929−932.
(18) Efros, Al. L.; Rosen, M.; Kuno, M.; Nirmal, M.; Norris, D. J.; Bawendi, M. Band-Edge Exciton in Quantum Dots of Semiconductors with a Degenerate Valence Band: Dark and Bright Exciton States. *Phys. Rev. B* **1996**, *54* (7), 4843−4856.
(19) Morgan, D. P.; Kelley, D. F. What Does the Transient Absorption Spectrum of CdSe Quantum Dots Measure? *J. Phys. Chem. C* **2020**, *124* (15), 8448−8455.
(20) Sercel, P. C.; Efros, A. L. Band-Edge Exciton in CdSe and Other II−VI and III−V Compound Semiconductor Nanocrystals − Revisited. *Nano Lett.* **2018**, *18* (7), 4061−4068.
(21) Vong, A. F.; Irgen-Gioro, S.; Wu, Y.; Weiss, E. A. Origin of Low Temperature *T*rion Emission in CdSe Nanoplatelets. *Nano Lett.* **2021**, *21* (23), 10040−10046.
(22) Pandya, R.; Steinmetz, V.; Puttisong, Y.; Dufour, M.; Chen, W. M.; Chen, R. Y. S.; Barisien, T.; Sharma, A.; Lakhwani, G.; Mitioglu, A.; et al. Fine Structure and Spin Dynamics of Linearly Polarized Indirect Excitons in Two-Dimensional CdSe/CdTe Colloidal Heterostructures. *ACS Nano* **2019**, *13* (9), 10140−10153.
(23) Norris, D. Electronic Structure in Semiconductor Nanocrystals. In *Nanocrystal Quantum Dots*, 2nd ed.; CRC Press: 2010; pp 63−96.
(24) Keene, J. D.; Freymeyer, N. J.; McBride, J. R.; Rosenthal, S. J. Ultrafast Spectroscopy Studies of Carrier Dynamics in Semiconductor Nanocrystals. *iScience* **2022**, *25* (2), No. 103831.
(25) Shockley, W.; Queisser, H. J. Detailed Balance Limit of Efficiency of *P-n* Junction Solar Cells. *J. Appl. Phys.* **1961**, *32* (3), 510−519.
(26) Nelson, C. A.; Monahan, N. R.; Zhu, X.-Y. Exceeding the Shockley−Queisser Limit in Solar Energy Conversion. *Energy Environ. Sci.* **2013**, *6* (12), 3508.
(27) Ross, R. T.; Nozik, A. J. Efficiency of Hot-carrier Solar Energy Converters. *J. Appl. Phys.* **1982**, *53* (5), 3813−3818.
(28) Yu, X.-Y.; Liao, J.-Y.; Qiu, K.-Q.; Kuang, D.-B.; Su, C.-Y. Dynamic Study of Highly Efficient CdS/CdSe Quantum Dot-Sensitized Solar Cells Fabricated by Electrodeposition. *ACS Nano* **2011**, *5* (12), 9494−9500.
(29) Yu, J.; Chen, R. Optical Properties and Applications of Two-dimensional CdSe Nanoplatelets. *InfoMat* **2020**, *2* (5), 905−927.
(30) Sippel, P.; Albrecht, W.; van der Bok, J. C.; van Dijk-Moes, R. J. A.; Hannappel, T.; Eichberger, R.; Vanmaekelbergh, D. Femtosecond Cooling of Hot Electrons in CdSe Quantum-Well Platelets. *Nano Lett.* **2015**, *15* (4), 2409−2416.
(31) Wang, J.; Wang, L.; Yu, S.; Ding, T.; Xiang, D.; Wu, K. Spin Blockade and Phonon Bottleneck for Hot Electron Relaxation Observed in N-Doped Colloidal Quantum Dots. *Nat. Commun.* **2021**, *12* (1), 550.
(32) Hopper, T. R.; Gorodetsky, A.; Frost, J. M.; Müller, C.; Lovrincic, R.; Bakulin, A. A. Ultrafast Intraband Spectroscopy of Hot-Carrier Cooling in Lead-Halide Perovskites. *ACS Energy Lett.* **2018**, *3* (9), 2199−2205.
(33) Chen, J.; Messing, M. E.; Zheng, K.; Pullerits, T. Cation-Dependent Hot Carrier Cooling in Halide Perovskite Nanocrystals. *J. Am. Chem. Soc.* **2019**, *141* (8), 3532−3540.
(34) Li, M.; Bhaumik, S.; Goh, T. W.; Kumar, M. S.; Yantara, N.; Grätzel, M.; Mhaisalkar, S.; Mathews, N.; Sum, T. C. Slow Cooling and Highly Efficient Extraction of Hot Carriers in Colloidal Perovskite Nanocrystals. *Nat. Commun.* **2017**, *8* (1), No. 14350.
(35) Yang, Y.; Ostrowski, D. P.; France, R. M.; Zhu, K.; van de Lagemaat, J.; Luther, J. M.; Beard, M. C. Observation of a Hot-Phonon Bottleneck in Lead-Iodide Perovskites. *Nat. Photonics* **2016**, *10* (1), 53−59.
(36) Yang, J.; Wen, X.; Xia, H.; Sheng, R.; Ma, Q.; Kim, J.; Tapping, P.; Harada, T.; Kee, T. W.; Huang, F.; et al. Acoustic-Optical Phonon up-Conversion and Hot-Phonon Bottleneck in Lead-Halide Perovskites. *Nat. Commun.* **2017**, *8* (1), No. 14120.
(37) Roy, P.; Srivastava, S. K. In Situ Deposition of Sn-Doped CdS Thin Films by Chemical Bath Deposition and Their Characterization. *J. Phys. D Appl. Phys.* **2006**, *39* (22), 4771−4776.
(38) Tuinenga, C.; Jasinski, J.; Iwamoto, T.; Chikan, V. In Situ Observation of Heterogeneous Growth of CdSe Quantum Dots: Effect of Indium Doping on the Growth Kinetics. *ACS Nano* **2008**, *2* (7), 1411−1421.
(39) Perna, G.; Capozzi, V.; Minafra, A.; Pallara, M.; Ambrico, M. Effects of the Indium Doping on Structural and Optical Properties of CdSe Thin Films Deposited by Laser Ablation Technique. *European Physical Journal B* **2003**, *32* (3), 339−344.
(40) Wang, L.; Chen, Z.; Liang, G.; Li, Y.; Lai, R.; Ding, T.; Wu, K. Observation of a Phonon Bottleneck in Copper-Doped Colloidal Quantum Dots. *Nat. Commun.* **2019**, *10* (1), 4532.
(41) Lott, K.; Nirk, T.; Volobujeva, O.; Shinkarenko, S.; Türn, L.; Kallavus, U.; Grebennik, A.; Vishnjakov, A. High-Temperature Investigation of ZnS:Ga and CdSe:Ga. *Physica B: Condensed Matter* **2006**, *376*−*377*, 764−766.
(42) Yang, G.; Liu, L.; Shi, S.; Zhang, X.; Liang, Y.; Liang, G. Size-Dependent Auger Recombination in CdSe Quantum Dots Studied by Transient Absorption Spectroscopy. *Journal of the Chinese Chemical Society* **2021**, *68* (11), 2054−2059.
(43) Utterback, J. K.; Ruzicka, J. L.; Hamby, H.; Eaves, J. D.; Dukovic, G. Temperature-Dependent Transient Absorption Spectroscopy Elucidates Trapped-Hole Dynamics in CdS and CdSe Nanorods. *J. Phys. Chem. Lett.* **2019**, *10* (11), 2782−2787.
(44) Cumberland, S. L.; Hanif, K. M.; Javier, A.; Khitrov, G. A.; Strouse, G. F.; Woessner, S. M.; Yun, C. S. Inorganic Clusters as

Single-Source Precursors for Preparation of CdSe, ZnSe, and CdSe/ZnS Nanomaterials. *Chem. Mater.* **2002**, *14* (4), 1576−1584.
(45) Charalambidis, D.; Chikán, V.; Cormier, E.; Dombi, P.; Fülöp, J. A.; Janáky, C.; Kahaly, S.; Kalashnikov, M.; Kamperidis, C.; Kühn, S.; et al. *Extreme Light Infrastructure—Attosecond Light Pulse Source (ELI-ALPS) Project* **2017**, 181−218.
(46) Hädrich, S.; Shestaev, E.; Tschernajew, M.; Stutzki, F.; Walther, N.; Just, F.; Kienel, M.; Seres, I.; Jójárt, P.; Bengery, Z.; et al. Carrier-Envelope Phase Stable Few-Cycle Laser System Delivering More than 100 W, 1 MJ, Sub-2-Cycle Pulses. *Opt. Lett.* **2022**, *47* (6), 1537.
(47) Tauc, J.; Grigorovici, R.; Vancu, A. Optical Properties and Electronic Structure of Amorphous Germanium. *physica status solidi (b)* **1966**, *15* (2), 627−637.
(48) Roy, D.; Samu, G. F.; Hossain, M. K.; Janáky, C.; Rajeshwar, K. On the Measured Optical Bandgap Values of Inorganic Oxide Semiconductors for Solar Fuels Generation. *Catal. Today* **2018**, *300*, 136−144.
(49) Wang, C.; Wehrenberg, B. L.; Woo, C. Y.; Guyot-Sionnest, P. Light Emission and Amplification in Charged CdSe Quantum Dots. *J. Phys. Chem. B* **2004**, *108* (26), 9027−9031.
(50) Vishnu, E. K.; Kumar Nair, A. A.; Thomas, K. G. Core-Size-Dependent Trapping and Detrapping Dynamics in CdSe/CdS/ZnS Quantum Dots. *J. Phys. Chem. C* **2021**, *125* (46), 25706−25716.
(51) Cohn, A. W.; Rinehart, J. D.; Schimpf, A. M.; Weaver, A. L.; Gamelin, D. R. Size Dependence of Negative Trion Auger Recombination in Photodoped CdSe Nanocrystals. *Nano Lett.* **2014**, *14* (1), 353−358.
(52) Walker, G. W.; Sundar, V. C.; Rudzinski, C. M.; Wun, A. W.; Bawendi, M. G.; Nocera, D. G. Quantum-Dot Optical Temperature Probes. *Appl. Phys. Lett.* **2003**, *83* (17), 3555−3557.

https://doi.org/10.1021/acs.jpcc.3c04689
J. Phys. Chem. C 2024, 128, 3815−3823